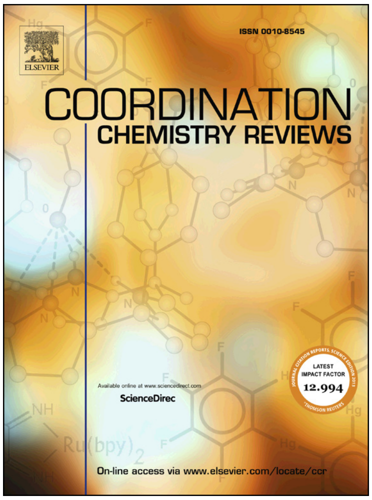

Review

Lanthanide-based self-assemblies of 2,6-pyridyldicarboxamide ligands: recent advances and applications as next-generation luminescent and magnetic materials

Jonathan A. Kitchen

PII: S0010-8545(17)30011-5
DOI: http://dx.doi.org/10.1016/j.ccr.2017.01.012
Reference: CCR 112386

To appear in: *Coordination Chemistry Reviews*

Received Date: 6 January 2017
Revised Date: 26 January 2017
Accepted Date: 26 January 2017

Please cite this article as: J.A. Kitchen, Lanthanide-based self-assemblies of 2,6-pyridyldicarboxamide ligands: recent advances and applications as next-generation luminescent and magnetic materials, *Coordination Chemistry Reviews* (2017), doi: http://dx.doi.org/10.1016/j.ccr.2017.01.012

Lanthanide-based self-assemblies of 2,6-pyridyldicarboxamide ligands: recent advances and applications as next-generation luminescent and magnetic materials

Jonathan A. Kitchen[a,*]

[a] Chemistry, University of Southampton, Highfield Campus, Southampton SO17 1BJ, United Kingdom
j.a.kitchen@soton.ac.uk

Abstract

The lanthanide-based coordination chemistry of ligands containing 2,6-pyridyldicarboxamide moieties over the last decade is reviewed. The review covers metallosupramolecular assemblies based on mononuclear, dinuclear and higher order systems.

Abbreviations: pdc, 2,6-pyridyldicarboxamide; dpa, 2,6-dipicolinic acid; SMM, Single Molecule Magnet; RCM, ring-closing metathesis; NMR, Nuclear Magnetic Resonance; CPL, Circularly Polarised Luminescence; MS, Mass Spectrometry; CD, Circular Dichroism; PEG, Polyethylene glycol; DMF, Dimethylformamide; SAXS, Small Angle X-ray Scattering; LB, Langmuir Blodgett; MRI, Magnetic Resonance Imaging.

Keywords: Lanthanide, 2,6-pyridyldicarboxamide, supramolecular, luminescence, self-assembly, magnetism

1. Introduction and background

The development of complex metallo-supramolecular architectures is an active and diverse research field, rich in fascinating chemistry with many potential applications.[1-7] Whilst historically this field has been heavily skewed towards transition metal-based systems, there is a smaller sub-section made up of lanthanide-based assemblies that have been the focal point for some research groups owing to their well-known optical and magnetic properties.[8-14] Moreover, with the current drive to develop more complex luminescent and magnetically interesting materials (*e.g.* luminescent cellular imaging systems, luminescent sensors, MRI contrast agents, Light Emitting Devices, Single Molecule Magnets (SMM) *etc.*) the use of Ln^{3+} ions in the assembly of complex, and functional, architectures has gained significant attention over the last decade or so.

When designing any functional supramolecular construct, careful consideration must be given to the components of the system. In the case of metallosupramolecular systems this refers to both the ligand and the metal centre. The hard Lewis acid nature and large coordination spheres (6-12 but often 8 or 9) of the lanthanides suggests ligands which are rich in oxygen and nitrogen donor atoms would make good building blocks for metallosupramolecular systems. Over the last few decades a large number of ligands that meet these criteria have been developed[15-23] however one of the most versatile and readily modified ligand scaffolds is that based on the terdentate 2,6-pyridyldicarboxamide (**pdc**) unit (Fig. 1). Their popularity arises in part because they are readily functionalised through simple and well-established chemistry (*e.g.* amide coupling) and also because they display predictable coordination to Ln^{3+} ions. In the majority of cases three **pdc** ligands coordinate one lanthanide ion to give 9 coordinate $[Ln(\textbf{pdc})_3]^{3+}$ species (*i.e.* a tris-mononuclear unit) with an N_3O_6 coordination sphere and a tri-capped trigonal prismatic geometry. Indeed, over the last decade a range of **pdc**-based ligands have been utilised to prepare Ln^{3+} assemblies with interesting and varied properties, which range from luminescent to magnetically interesting. In each case, the substituents were designed for structure directing properties, or were incorporated to enhance a specific property of the material (*e.g.* as an antenna or for surface attachment). Additionally, substituents were employed that allowed linking of multiple **pdc** moieties to form multi-topic ligands. The aim of this review is to highlight and discuss the recent advances in the development of Ln^{3+} directed assemblies that utilise the 2,6-pyridyldicarboxamide structural unit.

[Figure 1]

2. Mononuclear systems

Tris-mononuclear complexes of **pdc** represent the simplest of architectures discussed within the scope of this review, however, despite their apparent simplicity there have been many complex supramolecular assemblies developed. The following section highlights some of the systems developed over the last decade where the target compounds were tris-mononuclear complexes having the formula $[Ln(\mathbf{pdc})_3]^{3+}$.

*2.1 Tris-mononuclear complexes from symmetrical 2,6-substituted **pdc**-based ligands*

Ligand systems that incorporate the *same* amide substituent at the 2- and 6-position represent the simplest (from a synthetic perspective) of the **pdc**-based ligands. The simplest of the **pdc** ligands is the un-substituted pyridine-2,6-dicarboxamide [**L₁** (R_1 - R_5 = H)]. Complexes of Eu^{3+} and Tb^{3+} were prepared and structurally characterised by Tanase and co-workers.[24] In the solid state both complexes adopted the expected tri-capped trigonal prismatic coordination geometry where three **L₁** ligands complex to the lanthanide to give an N_3O_6 coordination sphere (Fig. 2). Importantly, the **pdc** ligand also effectively sensitises Eu^{3+} and Tb^{3+} emission in the solid state, highlighting the potential of **pdc** ligands for the development of luminescent lanthanide materials.

[Figure 2]

Following these un-substituted examples, a substantial variety of substituents have been incorporated into the **pdc** scaffold over the last decade using established amide coupling methodologies. These range from simple "non-functional" substituents (*e.g.* ethyl groups) through to those included for specific applications (*e.g.* trialkoxysilyl groups for Sol-Gel formation). In addition to amide substituents, the central 4-pyridyl position has also been functionalised to improve solubility characteristics, introduce additional antennae, and allow for material formation/immobilisation (*e.g.* gel formation).

The proven ability of **pdc** to coordinate and sensitise emission from visibly emitting lanthanides (namely Eu, Tb and Sm) has led researchers to incorporate the **pdc** moiety into systems for the design of macroscopic luminescent materials. One such example has been the incorporation of trialkyloxysilyl groups onto the scaffold of the **pdc**, giving rise to ligands, and subsequent coordination networks, which are capable of forming porous sol-gels *via* the polymerisation of the silyl groups. Alternatively, such groups can be used to form systems that can be immobilised onto surfaces.[25-29] For example, Barja and Aramendia used $\mathbf{L_2}$ (Fig. 3) to prepare a porous sol-gel network of Eu^{3+} complexes that acted as a sensor towards Cu^{2+}.[27] Using this same sol-gel approach, Wang and co-workers[25, 26] immobilised luminescent complexes of $[Ln(\mathbf{L_3})_3]$ into siloxane hybrid materials for sensing and imaging applications (Fig. 3).

[Figure 3]

In an effort to develop luminescent soft materials, Gunnlaugsson and co-workers designed a **pdc** derivative with additional coordination sites provided by functionalising the amide substituents. Specifically, $\mathbf{L_4}$ (Fig. 4) was designed to include peripheral carboxylate groups to act as secondary coordination sites for additional Ln^{3+} ions.[39] Addition of the first Ln^{3+} results in the formation of solution stable $[Ln(\mathbf{L_4})_3]^{3+}$ species where Ln^{3+} is bound in the central O_2N **pdc** pocket. When a second Ln^{3+} ion is added (either the same or different to the initial step), this binds to the peripheral COOH groups to form a cross-linked coordination polymer and the formation of a stable gel. By using mixed Ln^{3+} systems, the group were able to develop dual emissive gels containing Eu^{3+} and Tb^{3+}, which were observed to self-heal when swelled with methanol. Functional luminescent materials of this nature are highly sought after for the development of coatings and sensors.

[Figure 4]

The predictable self-assembly of **pdc** ligands with lanthanides to form tris-mononucelar complexes has also led to their use as templates for the formation of larger inter-locked architectures.[30, 31] Leigh and co-workers utilised $\mathbf{L_5}$, a **pdc**-based ligand where the amide substituents were terminated with alkene functional groups for subsequent use in ring-closing metathesis reactions (RCM).[30] Complexation of $\mathbf{L_5}$ with Lu^{3+} or Eu^{3+} resulted in the formation of the tris mononuclear complex $[Ln(\mathbf{L_5})_3]^{3+}$, with the alkene groups present on the periphery of the ligands well positioned for RCM (Fig 5). Indeed, treatment of the tris-templated system with a second-generation Hoveyda-Grubbs catalyst yielded an interlocked molecular trefoil knot containing a central 9-coordinate Ln^{3+} ion.

[Figure 5]

During the same year the group of Gunnlaugsson developed [2]- and [3]catenanes using lanthanide templates with a **pdc** based ligand, $\mathbf{L_6}$ (Fig. 6).[31] Unlike the system of Leigh, they did not include aromatic groups and opted for flexible alkene terminated polyethylene glycol (PEG) chains. Analogous to the synthetic approach used by Leigh *et al.*, synthesis was achieved by the formation of the luminescent tris-mononuclear Eu^{3+} complex [Eu(**L$_6$**)$_3$]$^{3+}$, before addition of 2nd generation Grubbs catalyst to effect the ring closure. Analysis of the reaction mixture by mass spectrometry revealed both the [2]catenane and the [3]catenane were present. These two studies showcase the use of the **pdc** moiety for the templated synthesis of large, interlocked molecules. Such systems are attractive research targets as they combine the interesting physical properties of the lanthanides with the synthetic complexity and versatility of interlocked supramolecular architectures.

[Figure 6]

Self-assembled Ln^{3+} systems that contain chiral ligands are able to exhibit Circularly Polarised Luminescence (CPL). Ln^{3+} systems in particular have excellent CPL properties with respect to imaging applications, and this has led to systems based on **pdc** ligands being investigated as chiroptical imaging probes. Muller and co-workers first introduced chirality into **pdc** ligands *via* amine coupling reactions, resulting in the enantiopure ligands ***RR*-L$_7$** and ***SS*-L$_7$** (Fig. 7). [32, 33] Both ***RR*-L$_7$** and ***SS*-L$_7$** readily formed tris-mononuclear complexes [Ln(**L$_7$**)$_3$]$^{3+}$ (Ln = Eu, Gd, Tb, and Yb) in solution which were stable over several months. The chiral nature of the assemblies was probed through CPL studies where the [Eu(**L$_7$**)$_3$]$^{3+}$ complexes displayed good Eu^{3+} centred CPL with differential emission intensities observed for [Eu(***RR*-L$_7$**)$_3$]$^{3+}$ and [Eu(***SS*-L$_7$**)$_3$]$^{3+}$. The researchers proposed that the direction that light is polarised is dependent on the helicity at the Eu^{3+}, which is in turn controlled by the absolute configuration of the chiral centre in the ligand – this was confirmed by the lack of a CPL signal from the racemic Eu^{3+} complex [Eu(***RS*-L$_7$**)$_3$]$^{3+}$. These advantageous properties (*i.e.* strong CPL, simple preparation and high stability) highlight the potential for such systems to be used as probes for chiral recognition.

[Figure 7]

Gunnlaugsson and co-workers have also been highly active in the development of chiral Ln^{3+} supramolecular architectures, and over the last decade they have developed a range of ligands for the development of such assemblies.[16, 34-40] The first examples of chiral **pdc** ligands from the Gunnlaugsson group were ***RR*-L₈** and ***SS*-L₈** (Fig. 8) with chiral naphthalene antenna groups on each of the amides (naphthalene was chosen as it is an ideal chromophore for Eu^{3+} sensitisation).[40]

[Figure 8]

Detailed self-assembly studies revealed the stable formation of the $[Ln(\mathbf{L_8})_3]^{3+}$ (Ln = Eu, Tb, Sm and Nd] complexes in solution. Structural studies were also carried out and revealed a "ball-like" nature of the complex where intramolecular π···π stacking between the coordinated pyridyl rings and the naphthalene antenna gave a tightly packed complex that resembled a ball (hence the complexes were dubbed the 'Trinity sliotar'). Analogous to the complexes of Muller, the 'sliotar' systems also displayed strong CPL in solution. The development of the Trinity sliotar was just the tip of the iceberg and over the last decade Gunnlaugsson and co-workers have extended this system to develop chiral Ln^{3+} coordination bundles.

[Figure 9]

The importance of ligand structure was investigated by preparing ligands ***RR*-L₉** and ***SS*-L₉** (Fig. 9). Here, the influence that the naphthalene substituent (*i.e.* positional isomer) had on the formation of the coordination bundles was investigated.[37, 38] Detailed solution and solid state studies were carried out by comparing the original sliotar systems $[Ln(\mathbf{L_8})_3]^{3+}$ to the new isomer $[Ln(\mathbf{L_9})_3]^{3+}$. Solution formation studies found that the latter ligands (***RR*-L₉** and ***SS*-L₉**) still formed the expected tris-mononuclear complexes, albeit with slightly lower formation constants. Crystallographic analysis of the complexes $[Eu(\boldsymbol{RR}\text{-}\mathbf{L_9})_3]^{3+}$ and $[Eu(\boldsymbol{SS}\text{-}\mathbf{L_9})_3]^{3+}$ and subsequent comparison to $[Eu(\boldsymbol{RR}\text{-}\mathbf{L_8})_3]^{3+}$ and

[Eu(***SS***-**L$_8$**)$_3$]$^{3+}$ revealed one major difference. The structures of [Eu(***RR***-**L$_9$**)$_3$]$^{3+}$ and [Eu(***SS***-**L$_9$**)$_3$]$^{3+}$ were more open and did not form the same tightly packed ball-like complexes, instead the 2-naphthalene groups were oriented away from the complex and do not involve π···π stacking to the same extent as in the complexes of [Eu(***RR***-**L$_8$**)$_3$]$^{3+}$ and [Eu(***SS***-**L$_8$**)$_3$]$^{3+}$ (Fig. 8). This study provided an excellent example of the importance of ligand choice when designing a supramolecular assembly as even seemingly subtle changes to the ligands can alter the structure of the metallosupramolecular construct obtained.

Based on the success of **pdc** ligands to reliably assemble enantioselective tris-mononuclear complexes (*i.e.* Δ or Λ at the lanthanide) where the handedness is dependent on the stereogenic centres in the ligand (*R* or *S*), the stereoselective synthesis of interlocked architectures has also been targeted. In an extension to their aforementioned molecular trefoil knot, Leigh and co-workers targeted the facile formation of enantiopure interlocked architectures by introduction of chiral substituents into the **pdc** ligand core (***SS***-**L$_{10}$** and ***RR***-**L$_{10}$**, Fig. 10).[41, 42] Like their previous systems, they were able to show that the assembly of the **pdc** ligand around a trivalent lanthanide, followed by RCM using a second generation Hoveyda-Grubbs catalyst, gave a molecular trefoil knot. Directed by the chirality of the **pdc** ligand, they were able to generate topologically chiral trefoil knots of single handedness.

[Figure 10]

Recently, this work has been extended to the stereoselective synthesis of a tied overhand knot from a **pdc**-based oligomer **L$_{11}$** (Fig. 11).[42]

[Figure 11]

However, as opposed to assembly from four components (1Ln and 3**pdc** ligands) they investigated a system where the three **pdc** motifs were linked together *via* flexible polyethylene glycol chains (**L$_{11}$**) which could assemble (tie) around Lu^{3+} and Eu^{3+}. Subsequent RCM on the terminal alkene units “tied” the system into a trefoil knot configuration. The inclusion of chiral groups in **L_{11}** allowed for specific helicity to be adopted by the lanthanide (as observed in many chiral **pdc** systems) and ultimately gave molecular knots of single handedness. The formation of such elegant supramolecular systems was contingent on the excellent coordination properties of the **pdc** core. Namely the ability for it to coordinate Ln^{3+} ions in a predictable manner and allow for adoption of specific helicity depending on the chirality the ligand possesses; and also its synthetic flexibility allowing for many complex components to be built into a simple ligand (*i.e.* allowing simple introduction of chiral components, incorporation of terminal alkenes for RCM, and the ability to form oligomers).

All of the complexes discussed up to this point contain **pdc** ligands modified on the amide arms. However, another method that researchers have used to alter the properties (photophysical and solubility) of **pdc** ligands, and the subsequent complexes, has been to modify the 4-position of the central pyridyl ring. In a study carried out by Maury and co-workers the 4-position was altered but the amides stayed the same. They showed the two-photon antenna effect in Eu^{3+} complexes of **L_{12}** and **L_{13}** (Fig. 12) ($[Eu(\mathbf{L_{12}})_3]^{3+}$ and $[Eu(\mathbf{L_{13}})_3]^{3+}$) where they could effect the efficient excitation of Eu^{3+} centred emission by changing the 4-substituent of the pyridine ring whilst keeping the amido substituents consistent.[43] The study was particularly important as it highlighted the influence of the 4-position in the manipulation of the properties of the ligands, and resulting complexes.

[Figure 12]

With the success of the Trinity Sliotar systems, and the reliable formation of tris-mononuclear complexes in solution, Gunnlaugsson and co-workers began to look towards additional applications. In attempts to move towards water-soluble systems, for applications as chiral cellular imaging probes, water solubilising groups were appended onto the periphery of the ligand in the form of short sulfonate terminated chains at the 4-position of the pyridyl ring to generate ***RR*-L_{14}** and ***SS*-L_{14}** (Fig. 13).[44]

[Figure 13]

The ligands were found to be water-soluble and able to form the expected tris complexes [Eu(***RR***-**L$_{14}$**)$_3$] and [Eu(***SS***-**L$_{14}$**)$_3$] in aqueous media at low concentrations. Unlike the systems described earlier, the sulfonate group renders the complex charge neutral. The [Eu(***RR***-**L$_{14}$**)$_3$] and [Eu(***SS***-**L$_{14}$**)$_3$] assemblies were again stable, and the ligand chirality responsible for directing the helicity of the metal centre giving rise to strong Eu^{3+} centred CPL emission. In an extension, the group investigated the formation of hydrogels of ***RR***-**L$_{14}$** and ***SS***-**L$_{14}$**. The ligands formed hydrogels in the presence of $CsCO_3$, however when Eu^{3+} was added to the gel mixture, precipitation of the neutral complex occurred and the gel network was disrupted. In order to overcome this, the group changed the SO^{3-} substituent to a neutral dimethylamine terminated chain and prepared soft materials (organogels) that exhibited logic functions when H$^+$ and F$^-$ were the inputs.[45]

2.2 – *Tris-mononuclear complexes from unsymmetrical 2,6-substituted* **pdc***-based ligands*

Alongside the development of **pdc** ligands that are symmetrically substituted at the 2- and 6-position, ligands for mononuclear complexes where the substituents differ have also been developed. In these systems the central coordination pocket is not significantly affected by appending different amide substituents (*i.e.* it is still an O_2N coordination pocket), however additional targeting and complexity can be introduced by the presence of multiple substituents. Synthetically, these ligands are more complex relative to the symmetric examples as there is a need to protect **one** of the carboxylate groups, whist leaving the other unprotected, before formation of the amide group can occur.

The group of Hamacek have developed many interesting **pdc**-based Ln^{3+} (*vide infra*) systems including a dual emissive Eu^{3+} assembly containing a tridentate ligand, **L$_{15}$**, which incorporates a central luminescent triangulenium dye moiety (Fig. 14).[46] Molecular modelling studies (in combination with poor quality X-ray diffraction data) suggested that the complex [Eu(**L$_{15}$**)]$^{4+}$ adopts a C$_3$ symmetrical arrangement where the three "arms" of the ligand curl upwards to coordinate the Eu^{3+} centre in a helical fashion (Fig. 14). This system highlighted the ability to incorporate additional functionality (*i.e.* a second luminophore) into **pdc** systems whilst still retaining the lanthanide coordination pocket. Such dual-emissive (bifunctional) systems have potential application as complex multimodal probes for biological and medical imaging.

[Figure 14]

Gunnlaugsson and co-workers have been instrumental in developing this field and over the last decade have developed many asymmetrically substituted **pdc** ligand systems. All of their systems retained one chiral naphthalene antenna (to induce specific helicity and allow for indirect excitation of the Eu^{3+} excited states) with, the other amide substituent chosen to impact specific additional functionality. One application targeted was the surface functionalization of CPL emitting species.[47] This was achieved by incorporation of a long alkyl chain ($C_{16}H_{33}$) on the amide substituent, for the purpose of forming Langmuir-Blodgett (LB) mono-layers on solid supports. The ligands ***R*-L$_{16}$** and ***S*-L$_{16}$** (Fig. 15) form the expected tris-mononuclear complexes [Eu(***R*-L$_{16}$**)$_3$]$^{3+}$ and [Eu(***S*-L$_{16}$**)$_3$]$^{3+}$ in solution and in the solid state. The complexes were found to be emissive and also display CPL where the point chirality at the ligand dictated the stereochemistry at the Eu^{3+} centre. Subsequently LB monolayers of [Eu(**L$_{16}$**)$_3$]$^{3+}$ were found to be emissive and retained their chirality upon deposition, giving rise to the first example of CPL from a lanthanide-based LB monolayer.

[Figure 15]

In follow-up studies, the group prepared NIR emitting [Nd(**L$_{16}$**)$_3$]$^{3+}$ LB films, and also investigated the effect of ligand structural isomerism on the formation of the LB films by utilising the isomeric [Eu(***R*-L$_{17}$**)$_3$]$^{3+}$ and [Eu(***S*-L$_{17}$**)$_3$]$^{3+}$ (Fig. 15) complexes where the systems also formed stable and emissive LB films with similar properties to those of [Eu(***R*-$\mathbf{L_{16}}$**)$_3$]$^{3+}$ and [Eu(***S*-$\mathbf{L_{16}}$**)$_3$]$^{3+}$.[48, 49] These systems were excellent examples of how rational ligand design can be applied to **pdc**-based systems for the targeting of specific applications, in this instance the incorporation of amphiphilicity for LB film formation.

3. Di-nuclear systems

The development of multi-nuclear metallosupramolecular architectures has fascinated chemists for many years. The formation of such complexes requires the design and synthesis of ligands that contain spacers of suitable length and rigidity to inhibit the ligand folding around the Ln^{3+} to form a mononuclear complex. In particular, di-nuclear helical structures are an attractive target for metallo-supramolecular chemists, in part owing to the similarity to complex self-assembled biological systems (*e.g.* the DNA helix).[50, 51] Thus ditopic **pdc**-based ligands have been used in conjunction with lanthanides to develop dinuclear triple-stranded helicates.

Dinuclear lanthanide systems using the bridged **pdc** ligand $\mathbf{L_{18}}$ (Fig. 16) were investigated by Hamacek and co-workers.[52] The ligand used in this study resulted in complex mixtures of dinuclear complexes in solution including [Ln$_2$($\mathbf{L_{18}}$)$_3$]$^{6+}$, [Ln$_2$($\mathbf{L_{18}}$)$_2$]$^{6+}$ and [Ln$_2$($\mathbf{L_{18}}$)]$^{6+}$ (Ln = La, Nd, Eu, Tb, Er and Lu). Interestingly, the group were able to isolate single crystals of the [Eu$_2$($\mathbf{L_{18}}$)$_2$]$^{6+}$ species and determine the molecular structure. In the solid state the complex adopted a dinuclear double-stranded helical arrangement where two $\mathbf{L_{18}}$ molecules coordinate two lanthanides with the remaining three binding sites on the lanthanides occupied by methanol solvent molecules to form [Eu$_2$($\mathbf{L_{18}}$)$_2$(MeOH)$_6$]$^{6+}$. The complex crystallises in a chiral space group, and although both *M*- and *P*- isomers are present, the *M*-helicate is the major contributor (87:13, *M*:*P*). As helicates are inherently chiral, mixtures of both isomers are often present and complexes are typically isolated as racemic mixtures of *M*- and *P*-helicates when achiral ligands are employed.[18, 53-57]

[Figure 16]

In efforts to synthesise enantioselective chiral helicates (*i.e.* selective formation of *M*- over *P*-helicates) Gunnlaugsson *et al.* developed chirally appended bridged ditopic **pdc** ligands to effect transfer of chirality from ligand to helix in the same way as the aforementioned "Trinity sliotar" mononuclear systems.[58-60] As for the sliotar systems, the naphthalene moiety was chosen not only as a source of point chirality, but also as an effective antenna for lanthanide excitation. The ligands $\mathbf{L_{19}}$, $\mathbf{L_{20}}$ and $\mathbf{L_{21}}$ (Fig. 17) were shown to self-assemble with Lu^{3+}, Eu^{3+}, Tb^{3+} and Sm^{3+} into stable, enantioselective di-lanthanide triple stranded helicates $[Ln_2(\mathbf{L_x})_3]^{6+}$ in solution. Transfer of chirality from ligand to metal was confirmed using CD spectroscopy and for $[Eu_2(\mathbf{L_x})_3]^{6+}$ CPL further confirmed that the point chirality on the ligand dictated the helicity adopted by the metal centre (ΛΛ for *R,R* and ΔΔ for *S,S*).

[Figure 17]

Law and co-workers reported further examples of dinuclear triple stranded helicates using the **pdc** ligands $\mathbf{L_{22}}$ and $\mathbf{L_{23}}$ (Fig. 18).[61] Both the *R,R* and *S,S* ligands were prepared with the position of the chiral centre at different distances from the **pdc** chelate pocket. The interaction of the ligands with either La^{3+} or Eu^{3+} resulted in the expected $[Ln_2(\mathbf{L_x})_3]^{6+}$ triple stranded helicates, however, despite the similar nature of the ligands, the products obtained were not the same. In the case of $\mathbf{L_{22}}$, the enantioselective synthesis of *M*- **or** *P*-helicates $[Ln_2(\mathbf{L_{22}})_3]^{6+}$ were observed depending on the point chirality at the ligand carbon atom (*R,R* gave the *M*-isomer and *S,S* gave the *P*-isomer). The interaction of $\mathbf{L_{23}}$ with La^{3+} or Eu^{3+} did not result in the same enantioselective synthesis, instead a mixture of *M*- **and** *P*-helicates was observed in a 1:1.1 ratio. This was an important structure-relationship study as it suggested a correlation existed between the position of the chiral centre (*i.e.* distance from the **pdc** group) and transfer of chirality from the ligand to metal centre. Such a study highlights the influence subtle changes in the ligand can have on the stereochemical selectivity of the resulting helix. Nevertheless, the **pdc** ligand was still coordinated to the lanthanide ions in the expected manner, and formed the triple stranded helicates in both solution and solid state.

[Figure 18]

Finally, bridging of two **pdc** units can occur at the central 4-pyridyl position rather than through the 2- or 6-amide substituents.[62] Ligand **L₂₄** (Fig. 19) is one such example of a ditopic ligand with Ln^{3+} binding sites linked in this manner. Rather than using **L₂₄** to self-assemble with free lanthanide ions, the researchers targeted the formation of dinuclear complexes where one **L₂₄** bridged two lanthanides that had previously been encapsulated in cyclen-based ligands (Tb·**1**). In the resulting complex, [**L₂₄**(Tb·**1**)₂], the **pdc** ligands effectively sensitised the characteristic green emission from the Tb^{3+} centres, which was absent in the precursor complex Tb·**1**. Displacement of **L₂₄** from [**L₂₄**(Tb·**1**)₂] was observed on exposure to a range of physiologically and biologically relevant anions. This manifested as a turn off of the Tb^{3+} centred emission demonstrating that [**L₂₄**(Tb·**1**)₂] can be used in a selective displacement assay for anion sensing where the selectivity was shown to follow the trend $H_2P_2O_7^{2-} > H_2PO_4^- > NO_3^- >>>$ Cl^- and CH_3COO^-.

[Figure 19]

4. Higher-order assemblies

Larger, more complex and arguably more impressive (from a structural perspective) supramolecular architectures have also been developed using multi-topic **pdc**-based ligands. Hamacek and co-workers have been particularly active in developing large supramolecular architectures using **pdc**-based ligands. Their initial studies focused on the tripodal ligand **L₂₅** (Fig. 20) that, in the presence of $Ln(ClO_4)_3$, self-assembled into a large tetranuclear helicate (tetrahedral cage) $[Ln_4(\mathbf{L_{25}})_4](ClO_4)_{12}$ (Fig. 20).[63-65]

[Figure 20]

The same group further expanded the tetranuclear helicates by adding an extra **pdc** coordination pocket to the tripodal ligand **L$_{25}$** to give the tetra-topic ligand **L$_{26}$** (Fig. 21).[66] Three equivalents of this large ligand species were able to arrange five lanthanide ions into a tower-like assembly that was capped with one equivalent of the tripodal ligand **L$_{26}$** (Fig 21). This system represented an excellent example of rational ligand design being used to isolate large assemblies in a predictable manner. This in part stemmed from the known coordination ability of **pdc**-based ligands when complexed with lanthanide ions.

[Figure 21]

In keeping with the penta-nuclear tower assembly mentioned above, Hamacek reported the preparation of the largest lanthanide **pdc** assembly to-date, where the hexatopic tripodal ligand **L$_{27}$** (Fig. 22) was used to prepare an octanuclear "expanded tetrahedral cage" assembly with Eu^{3+}.[67] The group used molecular modelling and small angle X-ray scattering (SAXS) to confirm the structure, which consisted of a central tetrahedral cage (akin to the aforementioned cages developed by Hamacek) however, each of the vertices was "expanded" with an additional europium to give the overall octanuclear assembly (somewhat resembling four dinuclear units arranged in a tetrahedron). Being able to take an already complex architecture (tetrahedral cage) and expand it predictably into an even more complex octanuclear assembly is testament to the ability of the **pdc** moiety to be used as a rational design tool for the "pre-programmed" development of large lanthanide-based architectures.

[Figure 22]

In 2015, Bünzli and co-workers developed the chiral ligands ***RR*-L$_{28}$**, ***SS*-L$_{28}$** and ***RRR*-L$_{29}$**, ***SSS*-L$_{29}$** (Fig. 23) for the stereoselective synthesis of tetrahedral cages.[68] The ligands differed in the number of **pdc** binding pockets with **L$_{28}$** containing two and **L$_{29}$** containing three. The assembly of these ligands with Eu^{3+} resulted in luminescent edge-capped $[Ln_4(\mathbf{L_{28}})_6]^{12+}$ and face-capped

$[Ln_4(\mathbf{L_{29}})_4]^{12+}$ tetrahedral cages respectively. With the inclusion of point chirality in the ligands, the cages were formed stereoselectivly as homochiral ΛΛΛΛ or ΔΔΔΔ cages. Chirality was confirmed by CD, NMR and in the case of $[Eu_4(\mathbf{L_{29}})_4](ClO_4)_{12}$ the molecular structure was determined. Interestingly, these architectures represented the first examples of stereoselective formation of Ln^{3+} tetrahedral cages, despite there being examples of many transition metal analogues.

[Figure 23]

The Ln^{3+} ions are also attractive for their magnetic properties, and Thomson, Konar and their respective co-workers reported examples of magnetically interesting lanthanide **pdc**-based systems.[69, 70] Thompson prepared the tri-topic ligands $\mathbf{L_{30}}$ - $\mathbf{L_{32}}$ (Fig. 24) and subsequently investigated the complxes formed with Dy^{3+}, La^{3+} and Gd^{3+} ions. The systems formed included helical tri-nuclear complexes of general formula $[Ln_3(\mathbf{L})_2(NO_3)_5(DMF)]$, with the Dy^{3+} system displaying single molecule magnet behaviour. Later, Konar prepared similar ligands ($\mathbf{L_{33}}$ and $\mathbf{L_{34}}$) that also gave helical tri-nuclear complexes and again the Dy^{3+} complex of $\mathbf{L_{33}}$ displayed SMM behaviour. To the best of our knowledge, these systems were the only examples of **pdc**-based molecular magnets reported in the last decade.

[Figure 24]

5. Conclusions

This short review has aimed to highlight some of the fascinating chemistry carried out using **pdc**-based ligands in combination with trivalent lanthanide ions over the last decade. From the research carried out it is clear that the **pdc**-

binding motif is a powerful unit for lanthanide-based metallosupramolecular chemistry. Not only is the binding mode to lanthanides reliable and predictable, but also **pdc**-based ligands are relatively straightforward to functionalise. This combination of favourable coordination properties *and* synthetic versatility has led to **pdc**-based ligands being used to generate a range of complex supramolecular architectures. One of the highlights of **pdc**-based ligands has been the rational design of ligand systems that are predisposed to form such complex supramolecular assemblies in a predictable manner. Such "pre-programming" of ligands is one of the reasons that **pdc**-based systems continue to attract attention from many of the worlds leading supramolecular groups. Moreover, with research groups having developed control over synthesis and assembly of **pdc** systems there will no doubt be a drive towards more complex applications (*e.g.* selective sensing, bio-imaging, magnetism, stereoselective synthesis, catalysis to name but a few). Because of the significant investment of research into the **pdc** moiety over the last decade (to which this review is dedicated), it appears to hold a place amongst lanthanide coordination chemistry analogous to that which the terpyridine motif holds amongst transition metal coordination chemistry. As such, it will continue to attract the attention of researchers for the development of bigger, more complex, and ultimately useable architectures with real-world application.

Acknowledgements

JAK thanks the University of Southampton for support of this work and Dr Kelly Kilpin for helpful discussions. JAK is also grateful for the support of the Directed Assembly Grand Challenge Network.

Funding

This work was supported by the Engineering and Physical Science Research Council (EPSRC) through grant references EP/N009185/1 and EP/K014382/1.

References

[1] D.J. Wales, J.A. Kitchen, Chem. Cent. J., 10 (2016) 72.
[2] S.J. Bradberry, A.J. Savyasachi, M. Martinez-Calvo, T. Gunnlaugsson, Coord. Chem. Rev., 273–274 (2014) 226-241.
[3] L.F. Lindoy, K.-M. Park, S.S. Lee, Chem. Soc. Rev., 42 (2013) 1713-1727.
[4] M. Albrecht, Chem. Soc. Rev., 27 (1998) 281-288.
[5] A. Winter, U.S. Schubert, Chem. Soc. Rev., 45 (2016) 5311-5357.
[6] J.A. Kitchen, P.A. Gale, Complexity of Supramolecular Assemblies, in: F.R. Keene (Ed.) Chirality in Supramolecular Assemblies: Causes and Consequences, John Wiley & Sons, Ltd, United Kingdom, 2017, pp. 94 - 141.
[7] J.P. Byrne, J.A. Kitchen, T. Gunnlaugsson, Chem. Soc. Rev., 43 (2014) 5302-5325.
[8] J.-C.G. Bünzli, Acc. Chem. Res., 39 (2006) 53-61.
[9] J.-C.G. Bunzli, S. Comby, A.-S. Chauvin, C.D.B. Vandevyver, J. Rare Earth, 25 (2007) 257-274.
[10] S.V. Eliseeva, J.-C.G. Bünzli, Chem. Soc. Rev., 39 (2010) 189-227.
[11] J.-C.G. Bünzli, Interface Focus, 3 (2013) 1 - 17.
[12] D.N. Woodruff, R.E.P. Winpenny, R.A. Layfield, Chem. Rev., 113 (2013) 5110-5148.
[13] S.J. Butler, D. Parker, Chem. Soc. Rev., 42 (2013) 1652-1666.
[14] D. Parker, Chem. Soc. Rev., 33 (2004) 156-165.
[15] D.E. Barry, D.F. Caffrey, T. Gunnlaugsson, Chem. Soc. Rev., 45 (2016) 3244-3274.
[16] C. Lincheneau, C. Destribats, D.E. Barry, J.A. Kitchen, R.D. Peacock, T. Gunnlaugsson, Dalton Trans., 40 (2011) 12056-12059.
[17] J.P. Byrne, J.A. Kitchen, J.E. O'Brien, R.D. Peacock, T. Gunnlaugsson, Inorg. Chem., 54 (2015) 1426-1439.
[18] N. Dalla-Favera, J. Hamacek, M. Borkovec, D. Jeannerat, F. Gumy, J.-C.G. Bünzli, G. Ercolani, C. Piguet, Chem. Eur. J., 14 (2008) 2994-3005.
[19] M. Albrecht, O. Osetska, J.-C.G. Bünzli, F. Gumy, R. Fröhlich, Chem. Eur. J., 15 (2009) 8791-8799.
[20] S. Zebret, N. Dupont, G. Bernardinelli, J. Hamacek, Chem. Eur. J., 15 (2009) 3355-3358.
[21] S.V. Eliseeva, O.V. Kotova, F. Gumy, S.N. Semenov, V.G. Kessler, L.S. Lepnev, J.-C.G. Buenzli, N.P. Kuzmina, J. Phys. Chem. A, 112 (2008) 3614-3626.
[22] S. Comby, S.A. Tuck, L.K. Truman, O. Kotova, T. Gunnlaugsson, Inorg. Chem., 51 (2012) 10158-10168.
[23] J.A. Kitchen, T. Gunnlaugsson, Supramolecular Chemistry: from sensors and Imaging Agents to Functional Mononuclear and Polynuclear Self-Assembly Lanthanide Complexes, in: D. A. Atwood (Ed.) The Rare Earth Elements, John Wiley & Sons Ltd., 2012, pp. 481-494.
[24] S. Tanase, P.M. Gallego, R. de Gelder, W.T. Fu, Inorg. Chim. Acta, 360 (2007) 102-108.
[25] Z. Zhou, Y. Zheng, Q. Wang, Inorg. Chem., 53 (2014) 1530-1536.
[26] Z. Zhou, Q. Wang, C.C. Zhang, J. Gao, Dalton Trans., 45 (2016) 7435-7442.
[27] B.C. Barja, P.F. Aramendia, Photochem. Photobiol. Sci., 7 (2008) 1391-1399.

[28] Z. Li, S. Zuo, J. Zhou, X. Yuan, Y. Song, H. Zhang, Chin. J. Chem., 33 (2015) 292-297.
[29] Y. Li, C. Wei, X. Wang, W. Sha, Y. Zhang, W. Jiang, Photochem. Photobiol., 87 (2011) 618-625.
[30] J.-F. Ayme, G. Gil-Ramirez, D.A. Leigh, J.-F. Lemonnier, A. Markevicius, C.A. Muryn, G. Zhang, J. Am. Chem. Soc., 136 (2014) 13142-13145.
[31] C. Lincheneau, B. Jean-Denis, T. Gunnlaugsson, Chem. Commun., 50 (2014) 2857-2860.
[32] F.C. Muller, G. Muller, J.P. Riehl, Chirality, 19 (2007) 826-832.
[33] K.N.T. Hua, J. Xu, E.E. Quiroz, S. Lopez, A.J. Ingram, V.A. Johnson, A.R. Tisch, A. de Bettencourt-Dias, D.A. Straus, G. Muller, Inorg. Chem., 51 (2012) 647-660.
[34] C. Lincheneau, J.P. Leonard, T. McCabe, T. Gunnlaugsson, Chem. Commun., 47 (2011) 7119-7121.
[35] C. Lincheneau, F. Stomeo, S. Comby, T. Gunnlaugsson, Aust. J. Chem., 64 (2011) 1315-1326.
[36] C. Lincheneau, R.M. Duke, T. Gunnlaugsson, Org. Biomol. Chem., 10 (2012) 6069-6073.
[37] O. Kotova, J.A. Kitchen, C. Lincheneau, R.D. Peacock, T. Gunnlaugsson, Chem. Eur. J., 19 (2013) 16181-16186.
[38] O. Kotova, S. Blasco, B. Twamley, J. O'Brien, R.D. Peacock, J.A. Kitchen, M. Martinez-Calvo, T. Gunnlaugsson, Chem. Sci., 6 (2015) 457-471.
[39] M. Martinez-Calvo, O. Kotova, M.E. Möbius, A.P. Bell, T. McCabe, J.J. Boland, T. Gunnlaugsson, J. Am. Chem. Soc., 137 (2015) 1983-1992.
[40] J.P. Leonard, P. Jensen, T. McCabe, J.E. O'Brien, R.D. Peacock, P.E. Kruger, T. Gunnlaugsson, J. Am. Chem. Soc., 129 (2007) 10986-10987.
[41] G. Zhang, G. Gil-Ramirez, A. Markevicius, C. Browne, I.J. Vitorica-Yrezabal, D.A. Leigh, J. Am. Chem. Soc., 137 (2015) 10437-10442.
[42] G. Gil-Ramirez, S. Hoekman, M.O. Kitching, D.A. Leigh, I.J. Vitorica-Yrezabal, G. Zhang, J. Am. Chem. Soc., 138 (2016) 13159-13162.
[43] A. Picot, F. Malvolti, B. Le Guennic, P.L. Baldeck, J.A.G. Williams, C. Andraud, O. Maury, Inorg. Chem., 46 (2007) 2659-2665.
[44] S.J. Bradberry, A.J. Savyasachi, R.D. Peacock, T. Gunnlaugsson, Faraday Discuss., 185 (2015) 413-431.
[45] S.J. Bradberry, J.P. Byrne, C.P. McCoy, T. Gunnlaugsson, Chem. Commun., 51 (2015) 16565-16568.
[46] J. Hamacek, C. Besnard, N. Mehanna, J. Lacour, Dalton Trans., 41 (2012) 6777-6782.
[47] J.A. Kitchen, D.E. Barry, L. Mercs, M. Albrecht, R.D. Peacock, T. Gunnlaugsson, Angew. Chem. Int. Ed., 51 (2012) 704-708.
[48] D.E. Barry, J.A. Kitchen, M. Albrecht, S. Faulkner, T. Gunnlaugsson, Langmuir, 29 (2013) 11506-11515.
[49] A. Galanti, O. Kotova, S. Blasco, C.J. Johnson, R.D. Peacock, S. Mills, J.J. Boland, M. Albrecht, T. Gunnlaugsson, Chem. Eur. J., 22 (2016) 9709-9723.
[50] M. Albrecht, Chem. Rev., 101 (2001) 3457-3498.
[51] M. Albrecht, Nat. Chem., 6 (2014) 761-762.
[52] B. El Aroussi, N. Dupont, G. Bernardinelli, J. Hamacek, Inorg. Chem., 49 (2010) 606-615.
[53] N. Andre, R. Scopelliti, G. Hopfgarter, C. Piguet, J.-C.G. Bünzli, Chem. Commun., (2002) 214-215.

[54] M. Albrecht, O. Osetska, R. Fröhlich, J.-C.G. Bünzli, A. Aebischer, F. Gumy, J. Hamacek, J. Am. Chem. Soc., 129 (2007) 14178-14179.

[55] C. Jia, B.P. Hay, R. Custelcean, Inorg. Chem., 53 (2014) 3893-3898.

[56] P.E. Ryan, L. Guenee, C. Piguet, Dalton Trans., 42 (2013) 11047-11055.

[57] J.-C.G. Buenzli, S. Petoud, C. Piguet, F. Renaud, J. Alloys Compd., 249 (1997) 14-24.

[58] S. Comby, F. Stomeo, C.P. McCoy, T. Gunnlaugsson, Helv. Chim. Acta, 92 (2009) 2461-2473.

[59] F. Stomeo, C. Lincheneau, J.P. Leonard, J.E. O'Brien, R.D. Peacock, C.P. McCoy, T. Gunnlaugsson, J. Am. Chem. Soc., 131 (2009) 9636-9637.

[60] C. Lincheneau, R.D. Peacock, T. Gunnlaugsson, Chem. Asian J., 5 (2010) 500-504.

[61] C.-T. Yeung, W.T.K. Chan, S.-C. Yan, K.-L. Yu, K.-H. Yim, W.-T. Wong, G.-L. Law, Chem. Commun., 51 (2015) 592-595.

[62] D.F. Caffrey, T. Gunnlaugsson, Dalton Trans., 43 (2014) 17964-17970.

[63] J. Hamacek, G. Bernardinelli, Y. Filinchuk, Eur. J. Inorg. Chem., (2008) 3419-3422.

[64] J. Hamacek, C. Besnard, T. Penhouet, P.-Y. Morgantini, Chem. - Eur. J., 17 (2011) 6753-6764.

[65] B. El Aroussi, L. Guenee, P. Pal, J. Hamacek, Inorg. Chem., 50 (2011) 8588-8597.

[66] B. El Aroussi, S. Zebret, C. Besnard, P. Perrottet, J. Hamacek, J. Am. Chem. Soc., 133 (2011) 10764-10767.

[67] S. Zebret, E. Vögele, T. Klumpler, J. Hamacek, Chem. Eur. J., 21 (2015) 6695-6699.

[68] L.-L. Yan, C.-H. Tan, G.-L. Zhang, L.-P. Zhou, J.-C. Bünzli, Q.-F. Sun, J. Am. Chem. Soc., 137 (2015) 8550-8555.

[69] M.U. Anwar, S.S. Tandon, L.N. Dawe, F. Habib, M. Murugesu, L.K. Thompson, Inorg. Chem., 51 (2012) 1028-1034.

[70] A. Adhikary, J.A. Sheikh, S. Biswas, S. Konar, Dalton Trans., 43 (2014) 9334-9343.

List of Figure Captions:

[Figure 1: Representation of the core structure of the **pdc** ligand system. Coordinating atoms highlighted in red.]

[Figure 2: Schematic of **L$_1$** (left) used by Tanase and co-workers to generate tris-mononuclear Eu^{3+} and Tb^{3+} and molecular structure showing the coordination mode of **L$_1$** with Eu^{3+} (Green = Ln^{3+}, Grey = C, Red = O and Blue = N)]

[Figure 3: **L$_2$** and **L$_3$** containing trialkyloxysilyl groups for materials applications (top). Schematic showing how complexes of **L$_3$** are immobilised onto surfaces, and image of emission from Eu^{3+} and Tb^{3+} systems (bottom). Reprinted with permission from [25]. Copyright 2014 American Chemical Society]

[Figure 4: **L$_4$** used by Gunnlaugsson and co-workers for developing coordination polymers (top). Schematic showing gel formation (A and B), gels on surfaces (C), emission profiles of Eu^{3+} and Tb^{3+} gels (D), emission profile for a mixed Eu^{3+}/Tb^{3+} gel (E). Reprinted with permission from [39]. Copyright 2015 American Chemical Society]

[Figure 5: **L$_5$** used by Leigh and co-workers for developing interlocked architectures and molecular structure of complex before RCM.]

[Figure 6: **L$_6$** used by Gunnlaugsson and co-workers for developing interlocked systems. Cartoon demonstrating the assembly process and subsequent RCM (clipping) to generate the [3]catenane. Reprinted from Ref. [31] with permission form the Royal Society of Chemistry.]

[Figure 7: **RR-L$_7$** and **SS-L$_7$** used by Muller and co-workers to generate chiral assemblies. Molecular structures of resulting Eu^{3+} complexes (Green = Ln^{3+}, Grey = C, Red = O and Blue = N) – figures with coloured strands are show to emphasise helicity at the metal centres]

[Figure 8: Ligands ***RR*-$\mathbf{L_8}$** and ***SS*-$\mathbf{L_8}$** and the molecular structure of the resulting Eu^{3+} 'sliotar' complex [Eu(***RR*-$\mathbf{L_8}$**)$_3$]$^{3+}$ in both ball and stick and space filling representations]

[Figure 9: Ligands ***RR*-$\mathbf{L_9}$** and ***SS*-$\mathbf{L_9}$** and the molecular structure of the resulting Eu^{3+} complex [Eu(***SS*-$\mathbf{L_9}$**)$_3$]$^{3+}$. In this complex the structure does not have the same 'ball-like' structure of the previous **$\mathbf{L_8}$** complex.]

[Figure 10: Ligands ***RR*-$\mathbf{L_{10}}$** and ***SS*-$\mathbf{L_{10}}$** and the molecular structure of the resulting Eu^{3+} complex after RCM (coloured strand show how the three ligands arrange).]

[Figure 11: Ligand **$\mathbf{L_{11}}$** used by Leigh and co-workers to tie a molecular knot and the molecular structure of the resulting Eu^{3+} complex after RCM.]

[Figure 12: **$\mathbf{L_{12}}$** and **$\mathbf{L_{13}}$** used by Maury and co-workers]

[Figure 13: Water soluble ligands ***RR*-$\mathbf{L_{14}}$** and ***SS*-$\mathbf{L_{14}}$** and emission spectral changes on addition of Eu^{3+} (top). Gelation behaviour of ligands in the presence of lanthanide salts (bottom). Reprinted from Ref. [44] with permission form the Royal Society of Chemistry.]

[Figure 14: Ligand **$\mathbf{L_{15}}$** used by Hamacek to generate a Eu^{3+} system that also contained a dye compound (left). Simulated structure of the Eu^{3+} complex of **$\mathbf{L_{15}}$** (right). Reprinted from Ref. [46] with permission form the Royal Society of Chemistry.]

[Figure 15: Amphiphilic ligands ***R*-$\mathbf{L_{16}}$** and ***S*-$\mathbf{L_{16}}$** and ***R*-$\mathbf{L_{17}}$** and ***S*-$\mathbf{L_{17}}$** used to generate LB films of chiral Ln^{3+} systems and schematic showing arrangement of LB films on solid substrates. From Ref. [49]. Copyright © 2016 WILEY-VCH Verlag GmbH & Co.]

[Figure 16: Ligand **L$_{18}$** used by Hamacek for the formation of dinuclear systems. Molecular structure of the $[Eu_2(\mathbf{L_{18}})_2(MeOH)_6]^{6+}$ complex. NB: methyl groups on coordinated methanol molecules removed for clarity.]

[Figure 17: Chiral ditopic ligands used by Gunnlaugsson and co-workers for the formation of dinuclear triple stranded helicates.]

[Figure 18: Chiral ditopic ligands ***RR*-L$_{22}$**, ***SS*-L$_{22}$**, ***RR*-L$_{23}$**, ***SS*-L$_{23}$** used by Law and co-workers for the formation of dinuclear triple stranded helicates and the molecular structures. In these system the position of the chiral point group had a major influence on the nature of the self-assembled products.]

[Figure 19: Displacement assay system based on **L$_{24}$** and a Tb^{3+} cyclen complex used by Caffrey and Gunnlagsson.]

[Figure 20: Tripodal ligand **L$_{25}$** used by Hamacek for the formation of tetranuclear helicates and molecular structure of $[Ln_4(\mathbf{L_{25}})_4]^{12+}$]

[Figure 21: tetra-topic ligand **L$_{26}$** for the formation of pentanuclear tower-like assemblies. Calculated structure of the heteroleptic complex $[Ln_5(\mathbf{L_{26}})_3(\mathbf{L_{25}})]^{15+}$ formed using **L$_{26}$** and **L$_{25}$**. Reprinted with permission from [66]. Copyright 2011 American Chemical Society]

[Figure 22: The largest **pdc** based ligand (**L$_{27}$**) developed to date with six **pdc** groups linked together. Calculated structure of the octa-nuclear “expanded tetrahedral cage” $[Ln_8(\mathbf{L_{28}})4]^{24+}$ assembly showing two perspectives. From Ref. [67]. Copyright © 2015 WILEY-VCH Verlag GmbH & Co.]

[Figure 23: Ligands ***RR*-L$_{28}$**, ***SS*-L$_{28}$**, ***RRR*-L$_{29}$**, ***SSS*-L$_{29}$** for the selective formation of homochiral cages. Representation of edge capped tetrahedron formed from **L$_{28}$** and face capped tetrahedron formed using **L$_{29}$**.]

[Figure 24: Multi-topic ligands **L_{30} - L_{34}.** Molecular structure of tri-nuclear linear Dy^{3+} helicate formed using **L_{33}**.]

Highlights

- 2,6-pyridyldicarboxamide ligands that form complexes with lanthanide ions are reviewed
- Mononuclear, dinuclear and higher-order assemblies can be formed
- Lanthanides give interesting optical and magnetic properties to the self-assemblies

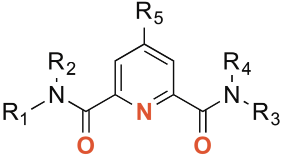
R5
R2
R4
N
N
N
R1
R3
O
O

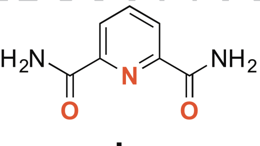

L_1

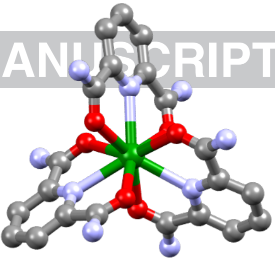

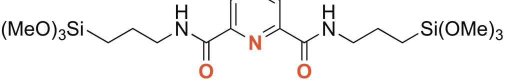
(MeO)$_3$Si
H
N
N
O
O
H
N
Si(OMe)$_3$

L$_2$

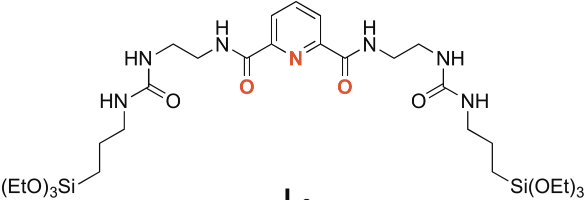
HN
H
N
N
O
O
H
N
NH
HN
O
O
NH
(EtO)$_3$Si
Si(OEt)$_3$

L$_3$

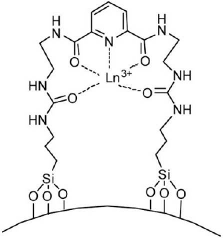
H
N
N
H
N
O
Ln^{3+}
O
NH
HN
O
O
HN
NH
Si
O
O
O
Si
O
O
O

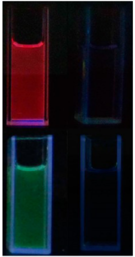

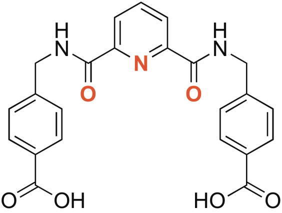
H
N
N
O
O
H
N
O
OH
HO
O

L_4

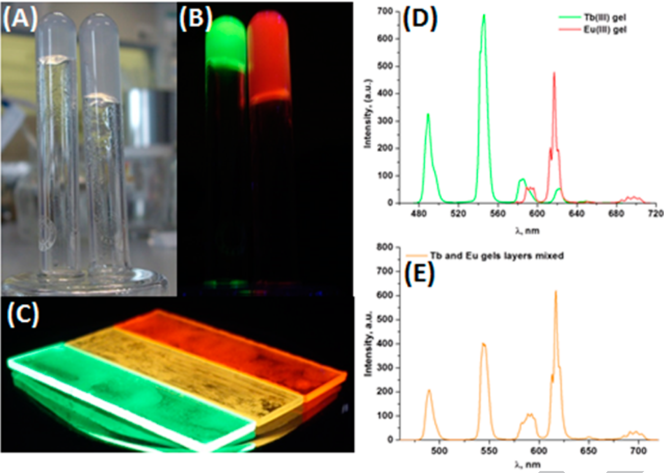
(A)
(B)
(C)
(D)
Tb(III) gel
Eu(III) gel
Intensity, (a.u.)
0
100
200
300
400
500
600
700
480
520
560
600
640
680
720
λ, nm
(E)
Tb and Eu gels layers mixed
Intensity, a.u.
0
100
200
300
400
500
600
700
800
500
550
600
650
700
λ, nm

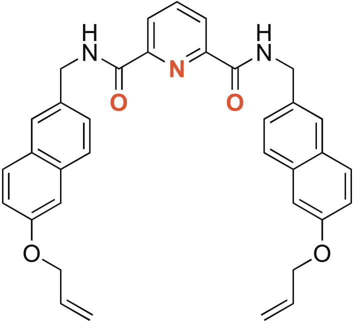

L_5

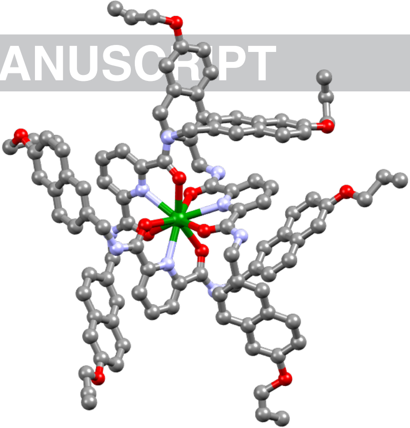

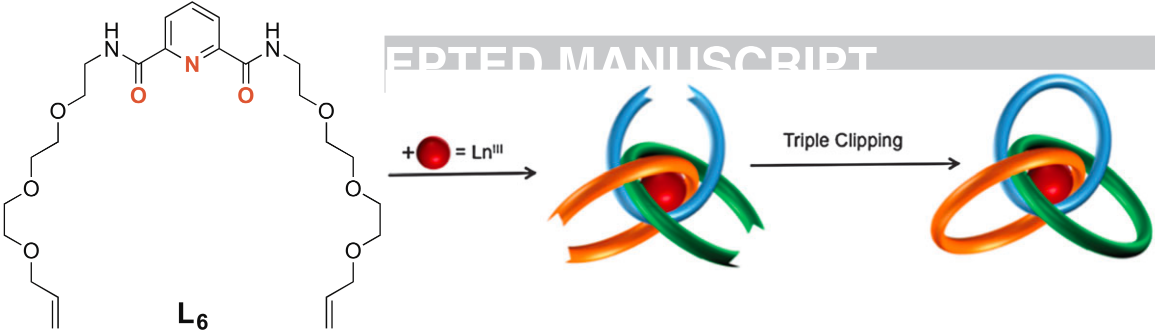
H
N
N
O
O
H
N
O
O
O
O
O
O
L_6
+ = Ln^{III}
Triple Clipping

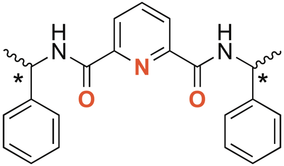

***RR*-L_7**
***SS*-L_7**

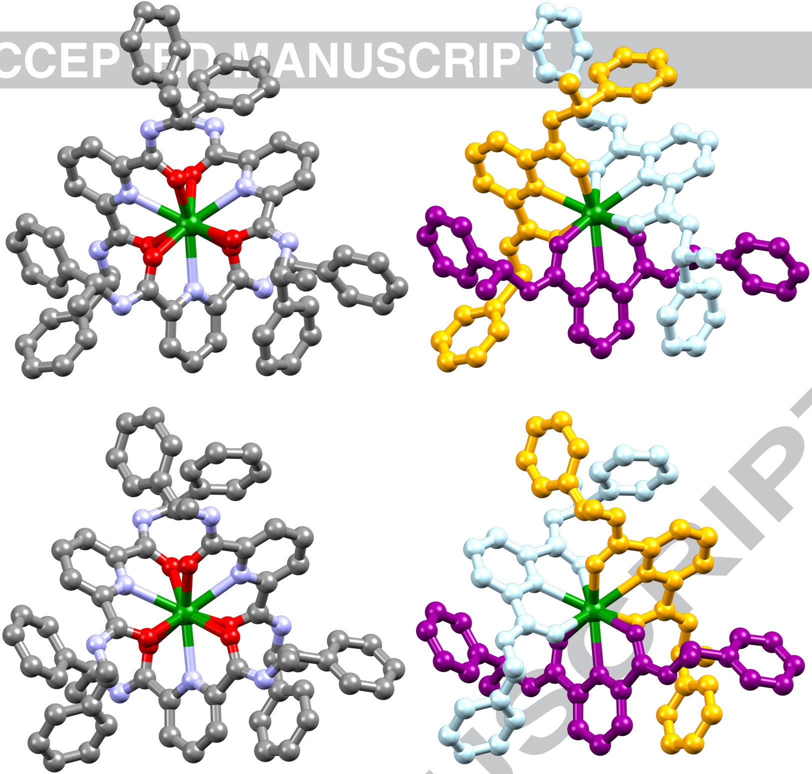

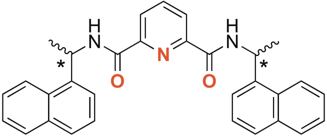

***RR*-L_8**
***SS*-L_8**

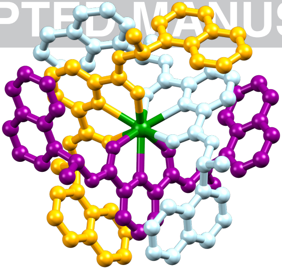

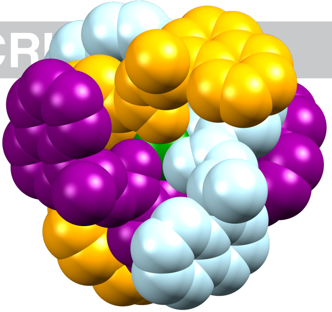

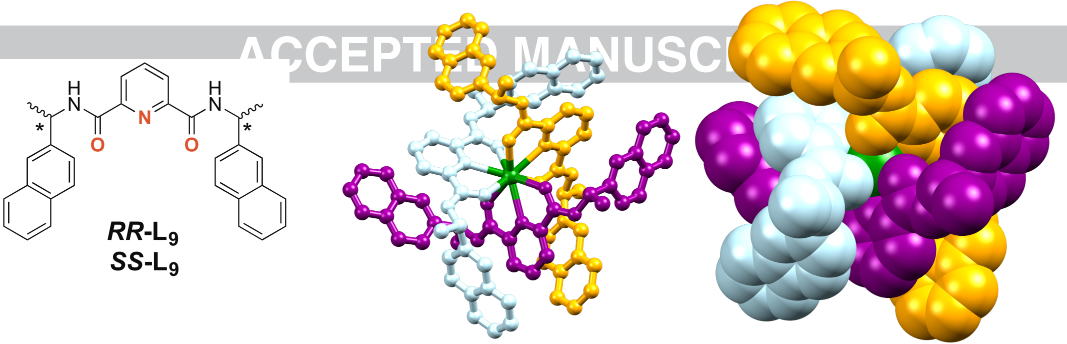

***RR*-L$_9$**
***SS*-L$_9$**

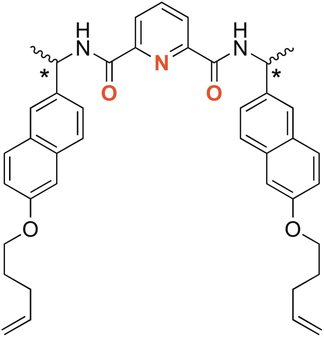

***RR*-L$_{10}$**
***SS*-L$_{10}$**

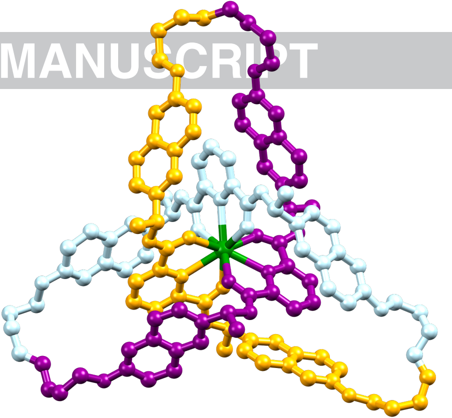

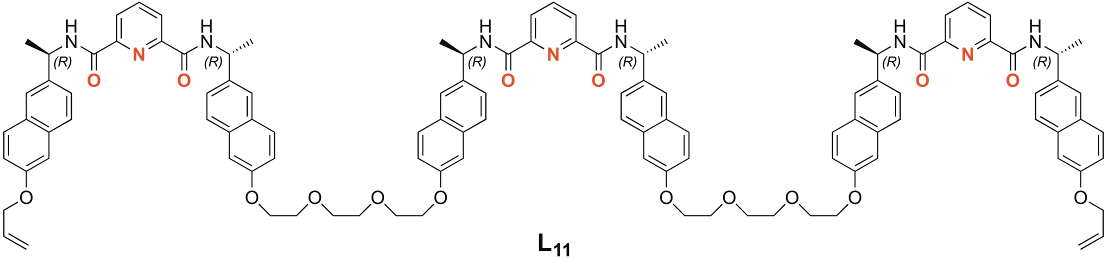

L_{11}

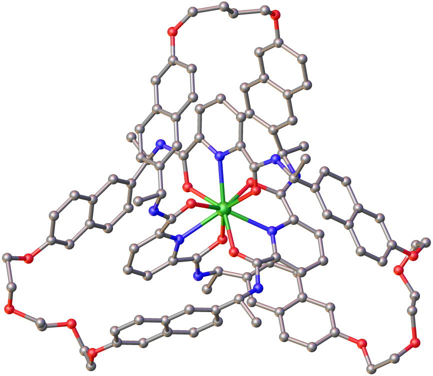

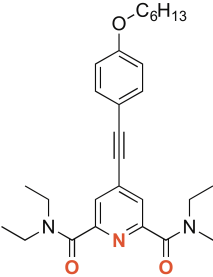

L_{12}

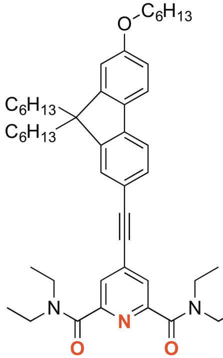

L_{13}

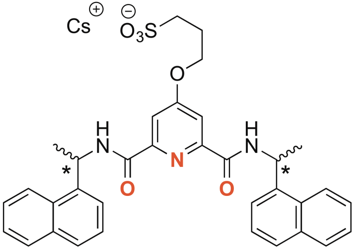

Cs⊕
⊖O3S
O
N
H N
N H
O
O
*
*

***RR*-L$_{14}$**
***SS*-L$_{14}$**

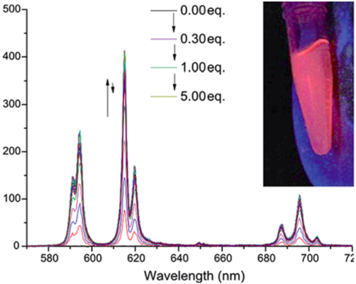

500
400
300
200
100
0
580
600
620
640
660
680
700
72
Wavelength (nm)
0.00eq.
0.30eq.
1.00eq.
5.00eq.

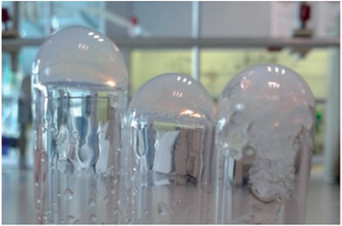

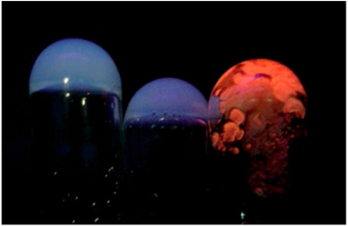

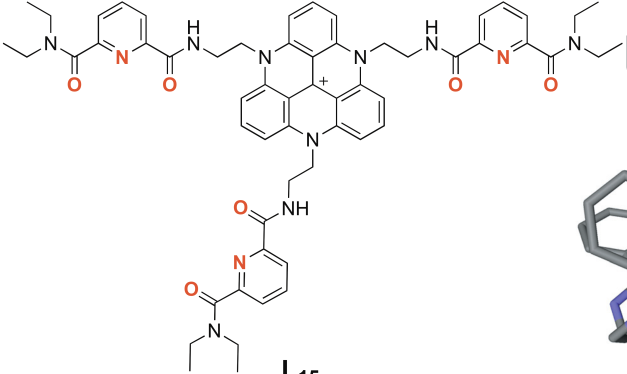

L_{15}

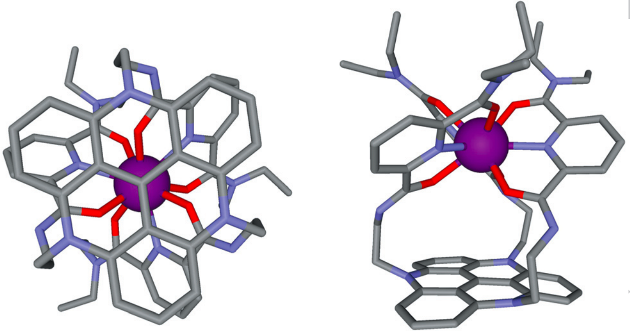

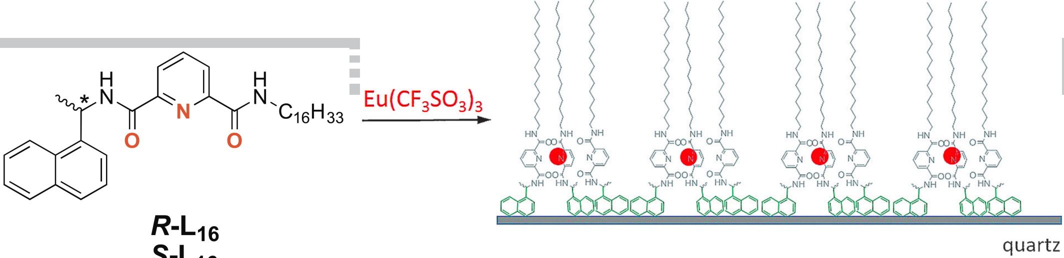

***R*-L$_{16}$**
***S*-L$_{16}$**

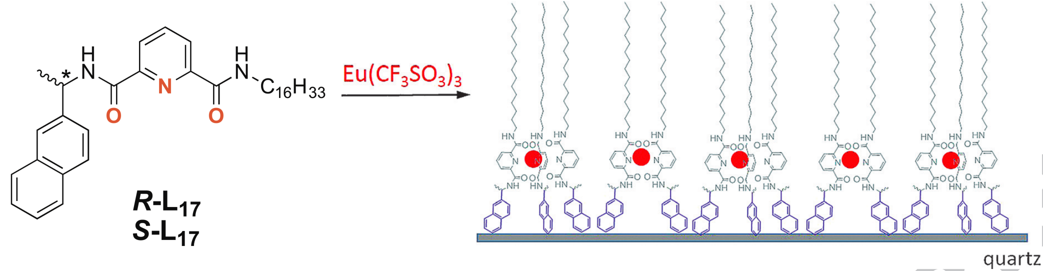

***R*-L$_{17}$**
***S*-L$_{17}$**

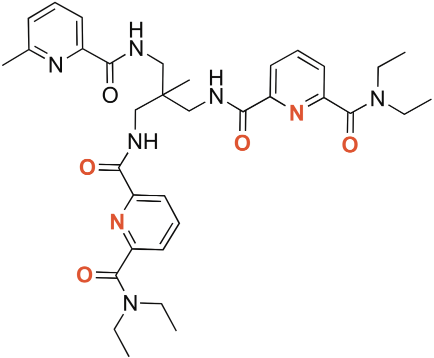

L_{18}

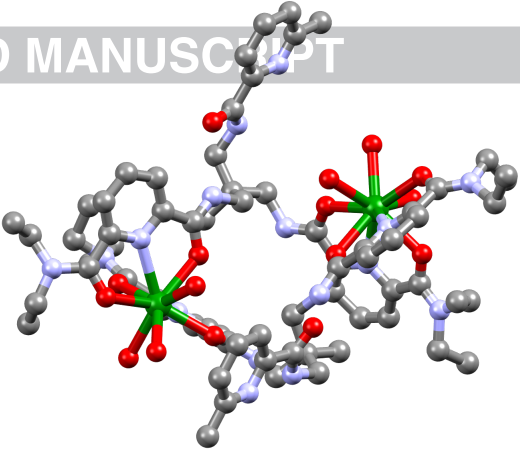

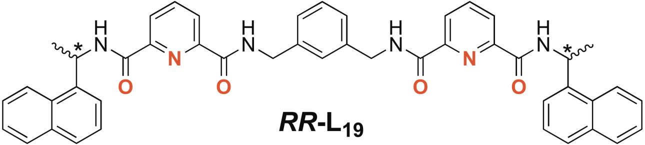

***RR*-L$_{19}$**

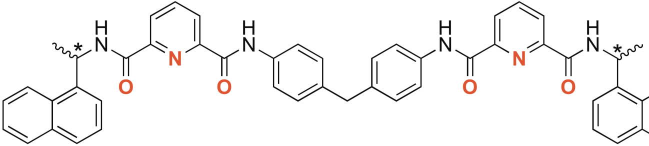

***RR*-L$_{20}$**
***SS*-L$_{20}$**

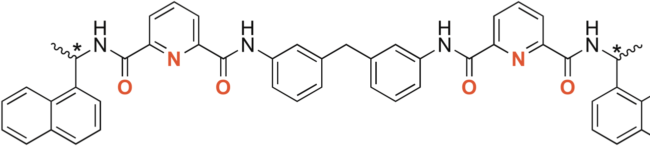

***RR*-L$_{21}$**
***SS*-L$_{21}$**

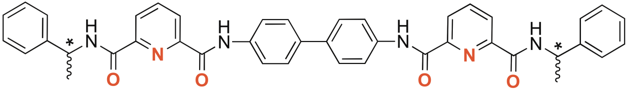

***RR*-L$_{22}$**
***SS*-L$_{22}$**

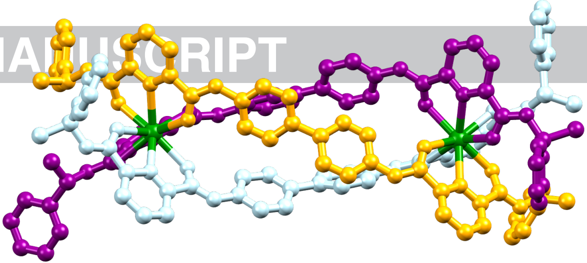

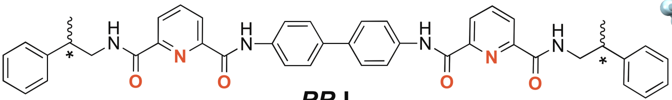

***RR*-L$_{23}$**
***SS*-L$_{23}$**

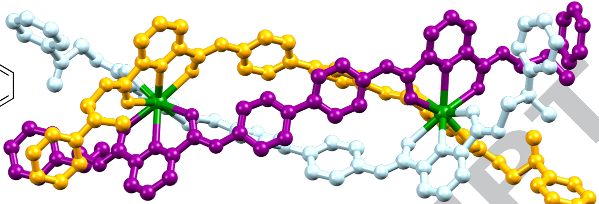

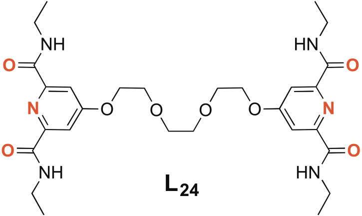

L_{24}

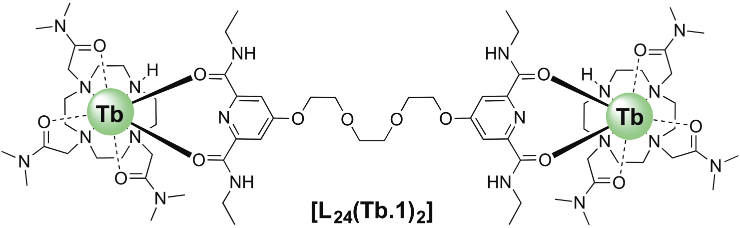

$[L_{24}(Tb.1)_2]$

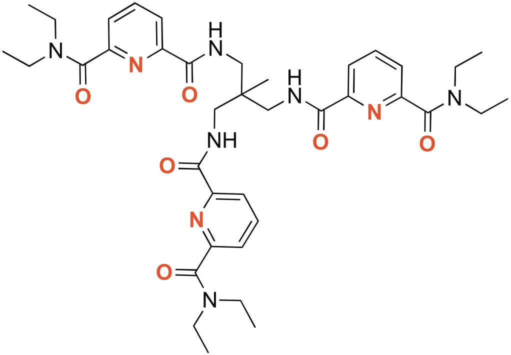

$\mathbf{L_{25}}$

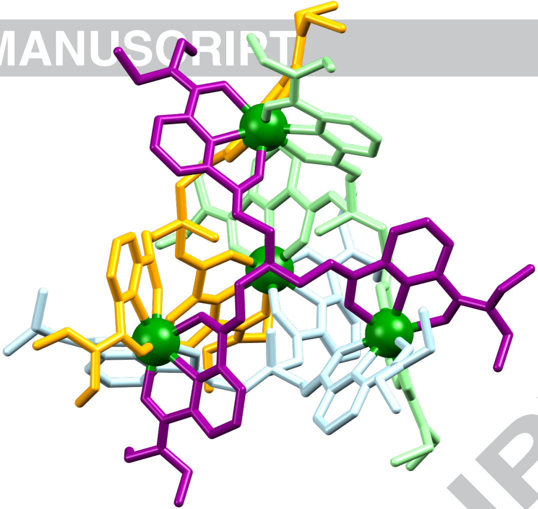

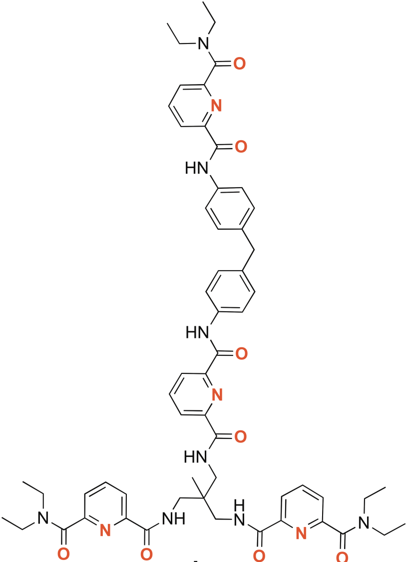

L_{26}

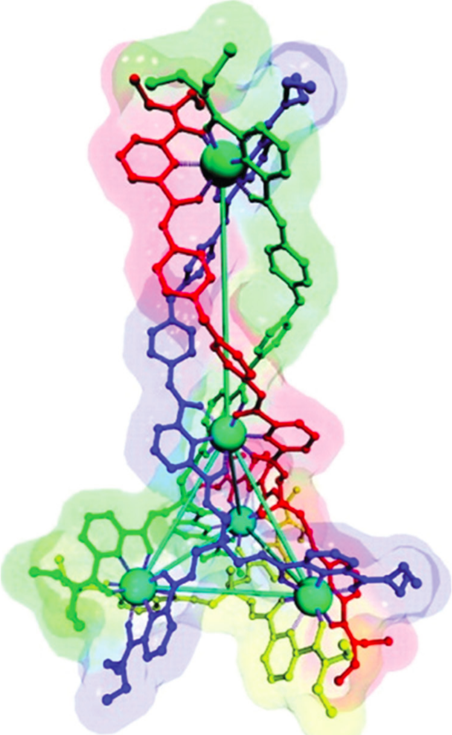

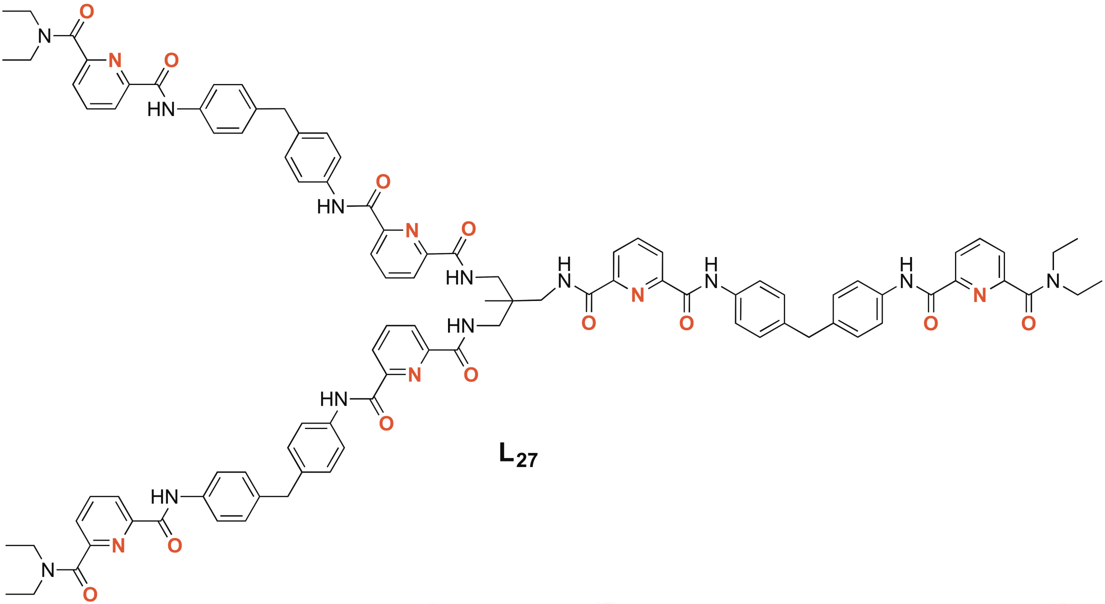

L_{27}

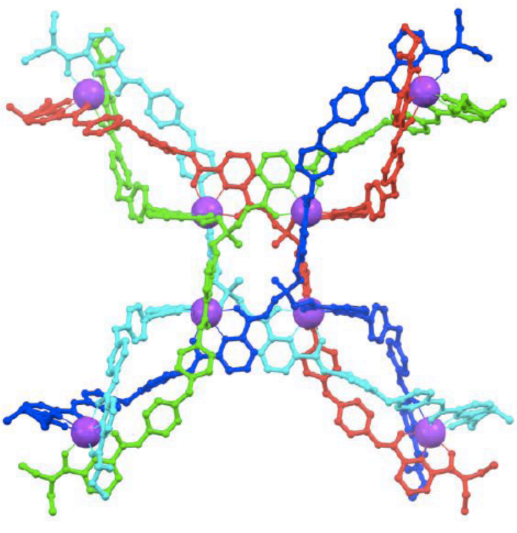

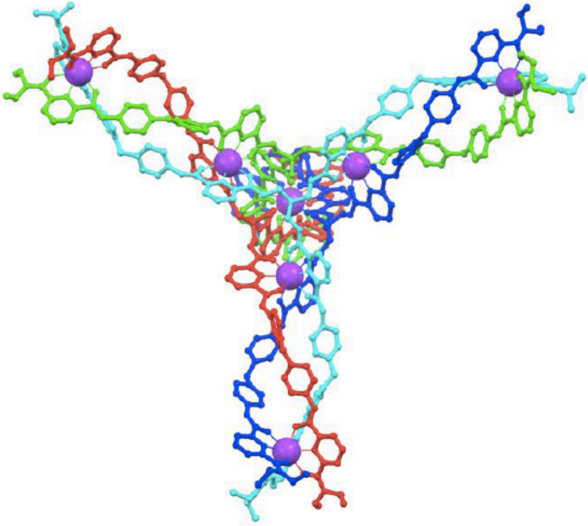

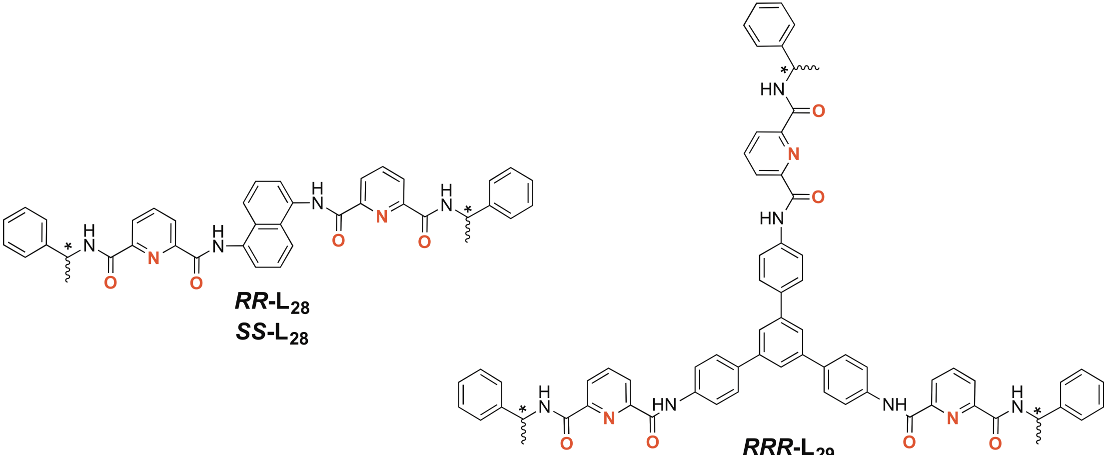

***RR*-L$_{28}$**
***SS*-L$_{28}$**

***RRR*-L$_{29}$**
***SSS*-L$_{29}$**

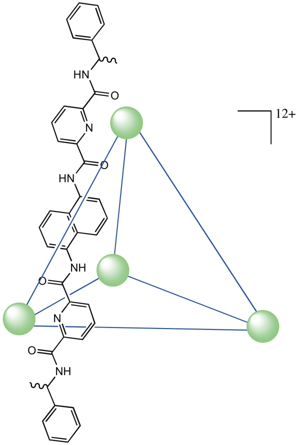

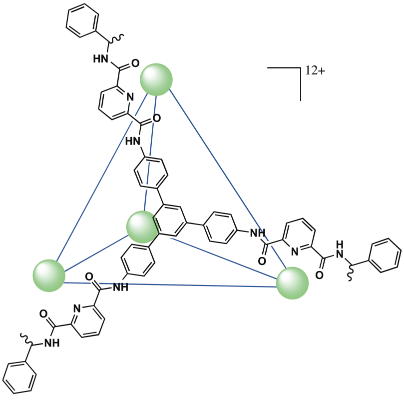

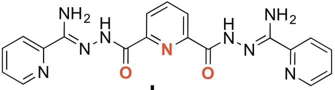

L30

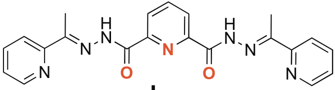

L31

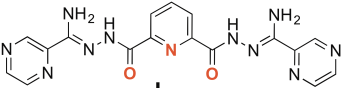

L32

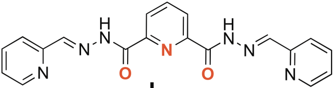

L33

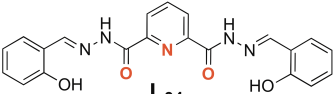

L34

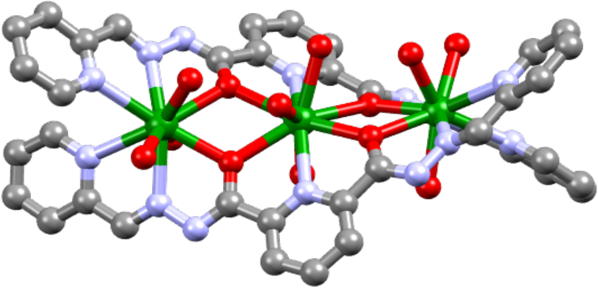

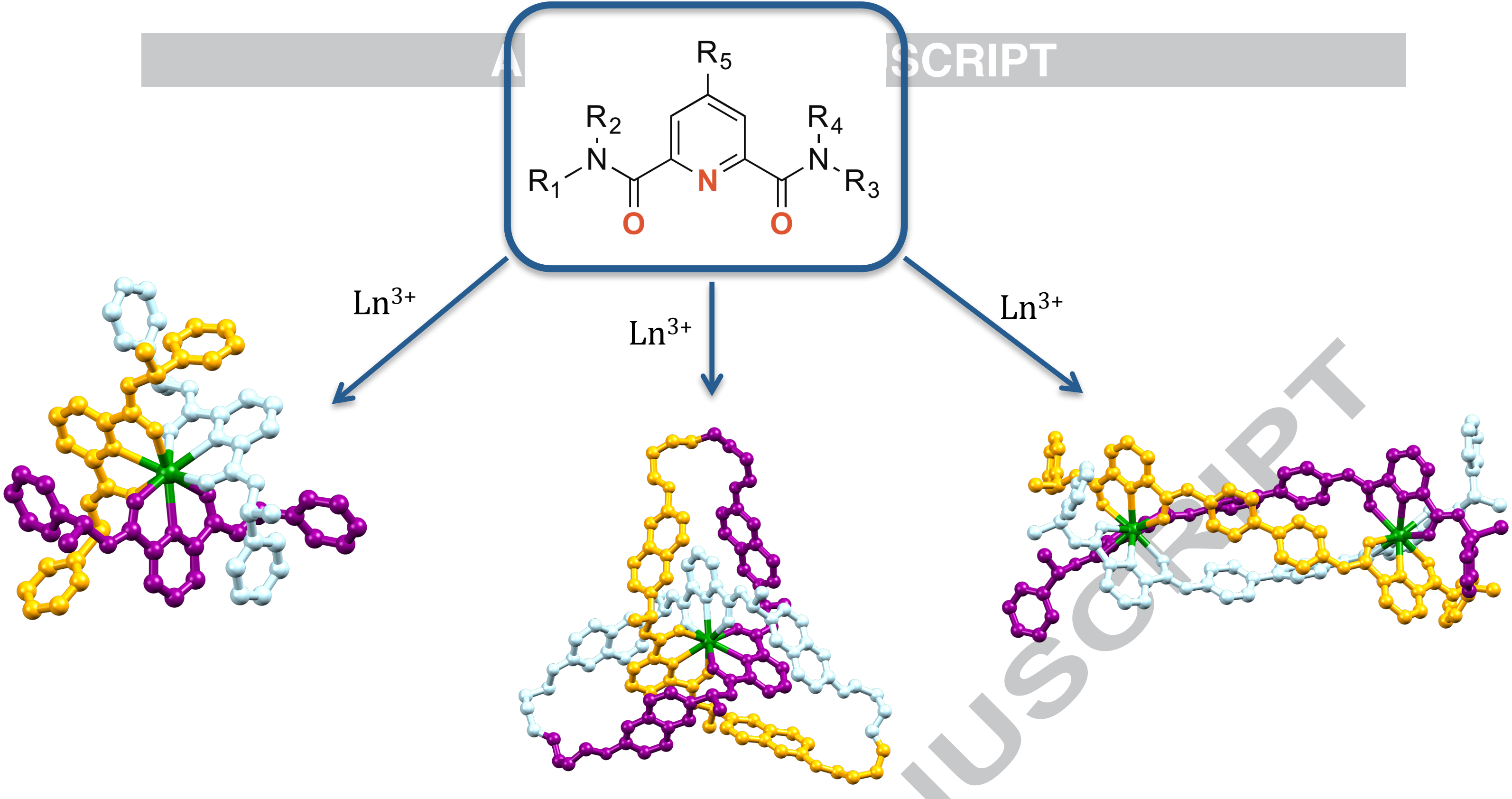
R_5
R_2
R_4
N
N
R_1
N
R_3
O
O
Ln^{3+}
Ln^{3+}
Ln^{3+}